Materials Science Forum Vol. 508 (2006) pp. 275-280
online at http://www.scientific.net

Liquid-Metal Foams – Feasible in-situ experiments under low gravity

N. Babcsán[1,2], F. Garcia-Moreno[1,2], D. Leitlmeier[3], J. Banhart[1,2]

1 Hahn-Meitner-Institute, SF3, Berlin, Germany

2 Technical University Berlin, Germany

3 ARC Leichtmetall-Kompetenzzentrum Ranshofen GmbH, Austria

babcsan@hmi.de

Keywords: metal foam, X-ray, radioscopy, low gravity.

Abstract. Metal foams are quite a challenge to materials scientists due to their difficult manufacturing. In all processes the foam develops in the liquid or semiliquid state. Liquid-metal foams are complex fluids which contain liquid metals, solid particles and gas bubbles at the same time. An X-ray transparent furnace was developed to monitor liquid metal foam evolution. Aluminium foams - similar to the commercial Metcomb® foams - were produced by feeding argon or air gas bubbles into an aluminium composite melt. The foam evolution was observed in-situ by X-ray radioscopy under normal gravity. Drainage and rupture were evaluated during the 5 min foam decay and 2 min solidification. Argon blown foams showed significant drainage and cell wall rupture during the first 20 s of foam decay. Air blown foams were stable and neither drainage nor rupture occurred. We demonstrated the feasibility of experiments during parabolic flight or drop tower campaigns. However, the development of a foam generator for low gravity is needed.

Introduction

Metal foams are a new challenging class of materials. One of them, the aluminium foam, is considered principally in future applications. Metal foams can be produced via baking compacted metal powders or creating bubbles in melts. Thus, the two routes are termed as *powder* or *melt,* respectively [1, 2]. One can easily memorize the former as “bread” and the latter as “beer” foam. In all processes the foam develops in the liquid or semi-liquid state. Liquid metal foams are complex fluids, which contain liquid metals, solid particles and gas bubbles at the same time. The foams of the powder route are fabricated by blowing in agents, creating the foam in a time scale of the order of minutes. Direct bubble input into the melt can accelerate the foam formation and decrease the foaming time to seconds.

In order to designan appropriate foam structure which meets industrial requirements, the foam evolution needs to be understood and controlled. Liquid metal foam evolution starts with formation, continues with decay and ends with solidification. All steps are affected by the stability of the foam. Phenomena related with aqueous foam stability are detailedly discussed in the literature in large monographs [3, 4, 5, 6] but only few publications relate to metal foams [7, 8, 9, 10].

The range of physical effects in liquid foams is wide, and they all influence one another as shown in Fig. 1. Here an arrow means that, e.g., drainage leads to coalescence, since it gradually reduces the thickness of films and therefore increases the probability for an instability which eventually destroys the films. The strategy in foam research is to eliminate some of these effects to be able to study the remaining ones. This is one motivation for using microgravity. In metallic foams, for example, there is little coarsening due to the inability of gas to diffuse through the relatively thick films; also, the flow of bubbles can be avoided by choosing stationary conditions in which foam expansion has come to an end. Therefore, microgravity is extremely valuable, allowing us to study coalescence phenomena without disturbing side effects. Coalescence is industrially relevant: it is a very strong effect in metallic foams and leads to a coarse and non-uniform pore structure and

inferior mechanical properties after solidification. Industry is therefore seeking methods to minimise coalescence, but up to present has not been very successful, since the underlying mechanisms are not understood.

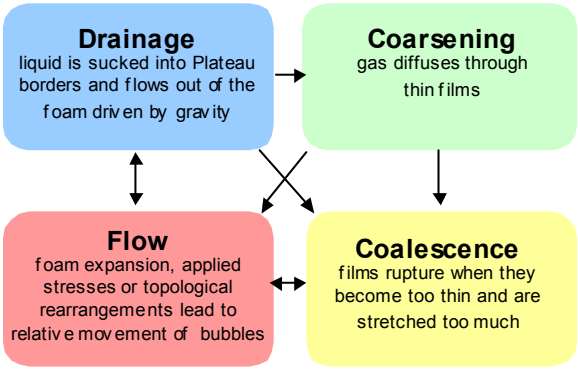

Fig.1. Interdependence of four principal phenomena in liquid foams.

In metal foams the phenomena related with foam stability can be studied ex-situ after solidification or in-situ during foaming. In 2003 García-Moreno et al. [11] developed a microfocus in-situ X-ray radioscopy scanner for monitoring metal foam evolution produced by the powder route. Previous techniques using synchrotron radiation were available [12]. For better understanding foam stability, a low gravity environment and in-situ monitoring of liquid metal foams have to be combined.

Former low gravity experiments on metal foams were performed in sounding rockets (CuSn in TEXUS 5, Al in TEXUS 3, 9, steel foam in TEXUS 4,6,7) [13] or parabolic flights (Pb foams) [10]. In all of them only ex-situ analysis of the samples were available. European Space Agency metal foams related activity [14] aims to carry out microgravity experiments on the International Space Station where in-situ analysis would be accessible both for the powder and the melt route [15]. Our activity is linked to this aim and plans to test X-ray monitoring of metal foam evolution in low gravity environment prior to the microgravity experiments. The efficiency of current microfocus sources and detectors which can be used during low gravity tests is limiting the range of metals to aluminium and aluminum alloys. The powder metallurgical foaming route is not sufficiently fast to carry out short duration experiments, but we demonstrated that this is feasible via the melt route.

Method

Particle stabilized aluminium foams were produced from a F3S20S Duralcan® metal matrix composite (MMC) precursor (Table 1) at 700°C. The foams were produced in an in-house assembled furnace using Metcomb® technology [16]. Bubbles of approximately 7 mm diameter in size were created on the bottom of the melt. Flow rate and gas pressure were controlled with a foam generator of HKB, Austria. The experiments were carried out using argon and air as foaming gases. Approximately 42 and 25 cm^3 foams were produced applying 4.2s (argon) and 2.5s (air) gas pulses, respectively. The temperature-time history of the experiments is shown in Fig. 2.

Table 1. Composition of the foam precursor

Name	Size, mm^3	Matrix					Particle	
		Al, wt%	Si, wt%	Fe, wt%	Cu, wt%	Mg, wt%	Amount, vol.%	Mean size, μm
F3S20S	16x37x37	Balance	9	0.16	<0.2	0.6	SiC, 20	10

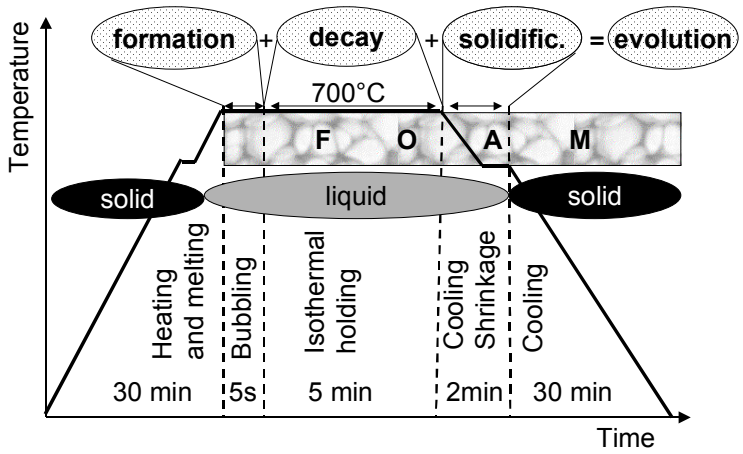

Fig. 2. Temperature-time history diagram of the foaming experiments

For an in-situ monitoring of the process a radioscopic X-ray scanner [11] was used. The foaming process can be recorded in-situ and in real time with frequencies of up to 9Hz and resolutions down to 5μm. The X-ray scanner consists of a Hamamatsu 150 kV microfocus X-ray source, a heating unit transparent to X-rays and a 2240 × 2368 pixels panel detector also from Hamamatsu. Magnifications up to 10 times can be obtained by varying the distances between source, sample and detector. During the recent experiments the parameters of the radioscopic unit were selected as 100 kV and 100 μA. The images during foam evolution were recorded with 1 frame per second using 3 times integration, 4x4 binning, 150 ms exposition time and 1.5x magnification. After the experiments the solid samples were photographed using 64 times integration, 1x1 binning, 150 ms exposition time and 1.02x magnification.

The image analyses of each individual picture were carried out by the software Axim. With help of the program we determined: a) the liquid volume distribution at the location of the foam and b) disappearing of clusters in comparison with the previous image. The former is utilized to draw density or drainage diagrams and the latter is taken for the accumulated rupture event diagrams.

Results

In spite of the considerable flow of bubbles during foam formation, foam rupture wasn't detected at this stage of the process. Characteristic images of foam evolution – recorded by the X-ray scanner – are shown in Fig. 3.a.b.c.e and Fig. 4.a.b.c.e. Fig. 3.d and Fig. 4.d display cross sections of the final solid foam samples in which the direction of the view is to the same as in the other parts of the figures. In Figs. 3 and 4 the images represent the argon- and the air-blown foam, respectively.

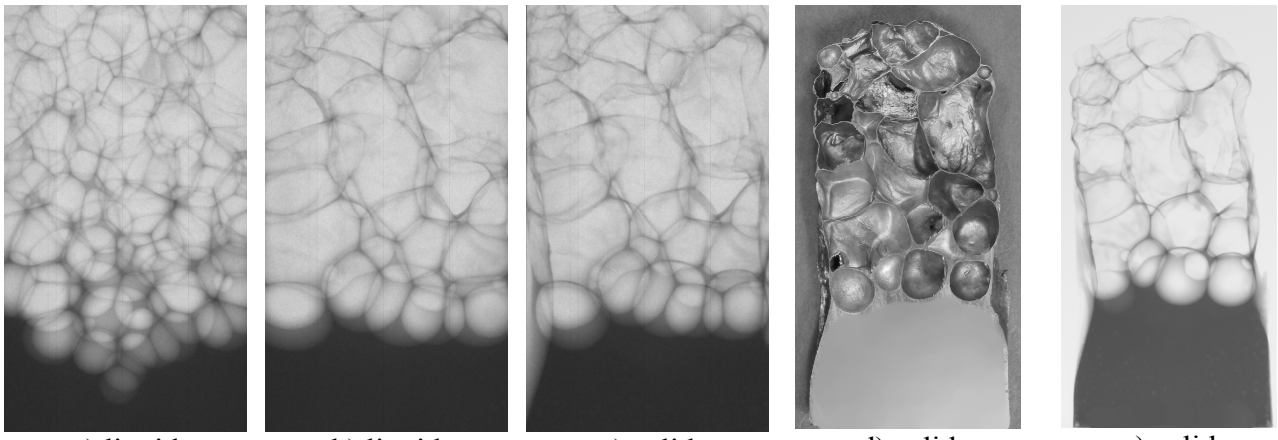

a) liquid b) liquid c) solid d) solid e) solid

Fig. 3. Evolution of *argon* blown foam: X-ray images a) just after foam formation b) at the end of isothermal holding c) at the end of solidification; d) half of the solid foam sample e) X-ray image of d. Sample widthis 40 mm at the bottom.

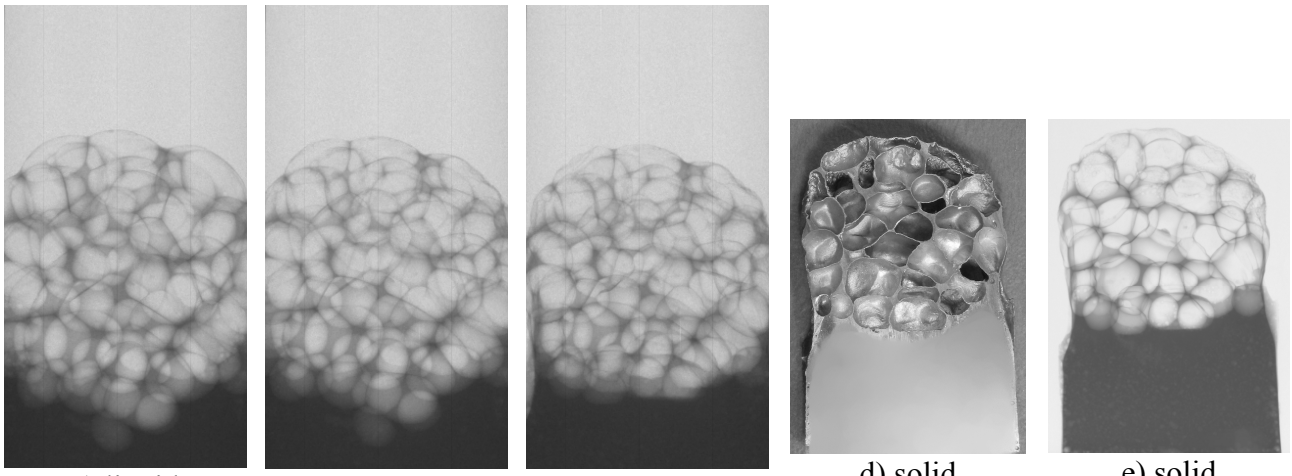

a) liquid b) liquid c) solid d) solid e) solid

Fig. 4. Evolution of *air* blown foam: X-ray images a) just after foam formation b) at the end of isothermal holding c) at the end of solidification;
d) half of the solid foam sample e) X-ray image of d. Sample widthis 40 mm at the bottom.

An accumulated rupture events diagram of argon blown foam is shown in Fig. 5. Air blown foam couldn't be evaluated because of a lack of rupturing events. Drainage curves of argon and air blown foams are shown in Figs. 6 and 7, respectively. In these figures Φ_l represents the liquid volume calculated from the horizontal pixel rows of the foam images.

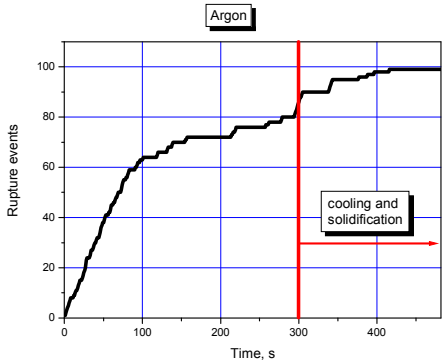

Fig. 5. Accumulated rupture events diagram of Argon blown foam

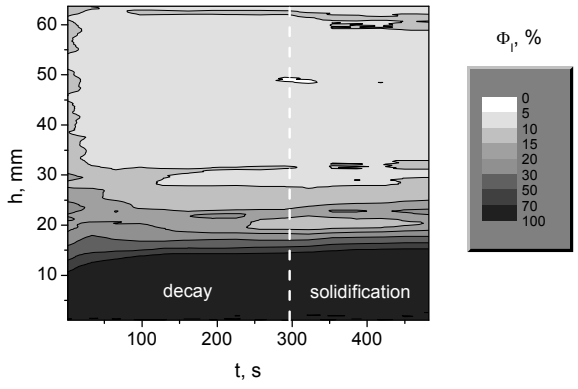

Fig. 6. Drainage curves of *argon* blown foam

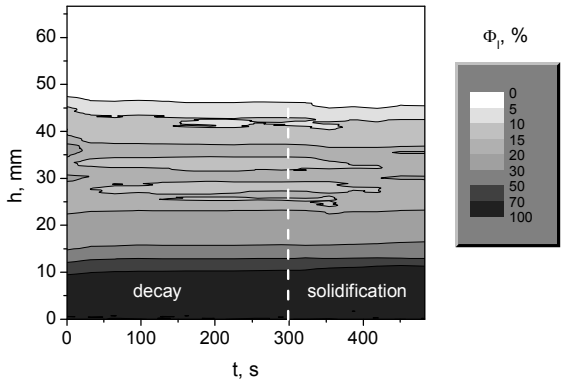

Fig. 7. Drainage curves of *air* blown foam

Discussion

Comparing Figs. 3.d and e, the most relevant characteristics that can be found on both the optical and the X-ray image, are the plateau borders. The reproducibility and the uniformity of the bubble sizes are clearly visible analysing and comparing Fig. 3.a and Fig. 4.a which are the images of the just created foams. Coalescence can be followed clearly in the argon blown foam, but not if air was applied as foaming gas (Fig. 3-5). During solidification the foam shrinks significantly in both cases (see Fig. 3.b-c and Fig. 4.b-c, respectively).

It is known from our previous ex-situ investigations [7] that a thick oxide skin develops on the inner surfaces of the cells. The thickness of the oxide skin is responsible for the stability of foams which is determined by the oxygen content of the foaming gases. Until now post-experimental analysis didn't reveal any information about early stages of foam decay. Freezing of liquid aluminium foams in less than one minute is difficult without destroying the foam structure. Using the in-situ technique significant drainage was found within the first 20 s of foam decay in the case of argon blown foam (Fig. 6). In air blown foam drainage was hardly detectable (Fig. 7). This difference can be explained using experimental results on single plateau borders of Koehler et al. [17] in aqueous foams. It was shown in this work that the mobility of surfaces of the foams determines the drainage rate. Immobile surfaces slow down drainage. Using the analogy with aqueous foams the oxide can be considered as an immobiliser of surfaces, thus leading to less drainage.

Conclusions

- In-situ monitoring of liquid metal foam evolution by X-ray radioscopy has been developed.
- Adaptation of the Metcomb® method results in short experimental times and a variability of the oxygen content of the foaming gas, which is difficult in the powder route.
- Liquid metal foams show significant drainage on earth in the first 20s of foam decay.
- Drainage and rupturing rate decrease with the oxygen content of the bubbling gas.
- It was demonstrated that in-situ low gravity experiments are feasible in liquid metal foams.

Acknowledgement

We wish to thank M. Fromme for developing the Axim software; H. Kropf, W. Rönnfeldt and T. Draxler for their technical assistance; F. Dobesberger and H. Flankl from HKB, Austria for the permission to publish this paper. The research was supported by ESA International Trainee grant and DFG Ba 1170/3-2.

References

[1] H. P. Degischer, B. Kriszt: *Handbook of cellular metals* (WILEY-VCH, Weinheim 2002)

[2] J. Banhart, D. Weaire, Physics Today Vol. 55 (July 2002) p. 37

[3] D. Weaire and S. Hutzler, The Physics of Foams, (Oxford University Press, Oxford 1999)

[4] J.J. Bikerman, *Foams*, (Springer-Verlag New York Inc., 1973)

[5] D. Exerowa and P.M. Kruglyakov, *Foam and foam films*, (Elsevier, 1998)

[6] P. R. Garrett, *Defoaming: theory and industrial application*, (Marcel Dekker Inc., New York 1993)

[7] N. Babcsán, D. Leitlmeier, H.-P. Degischer, J. Banhart, Adv. Eng. Mat., Vol.6 (2004), p. 421

[8] G. Kaptay, Colloids and Surfaces A 230 (2004) 67-80

[9] N. Babcsán, D. Leitlmeier and J. Banhart, Metal Foams – High Temperature Colloids, Colloids and Surfaces A, to be published

[10] Th. Wübben, H. Stanzik, J. Banhart and S. Odenbach, J. Phys.: Condens. Matter Vol. 15 (2003) p. 427

[11] F. Garcia-Moreno, M. Fromme, J. Banhart, in: J. Banhart, N.A. Fleck, A. Mortensen [Eds.], *Cellular Metals: Manufacture, Properties, Applications*, MIT-Verlag (2003) p. 89

[12] J. Banhart, H. Stanzick, L. Helfen, T. Baumbach, Applied Physics Letters Vol. 78 (2001) p. 1152

[13] European Space Agency: Erasmus Experiment Archive, http://spaceflight.esa.int/eea

[14] J. Banhart, μg-Foam, ESA project (AO-99-075)

[15] J. Banhart, in: D. Weaire and J. Banhart [Eds.], *Foams and Films*, MIT-Verlag Bremen (1999) p. 73

[16] D. Leitlmeier, H.P. Degischer and H.J. Flankl: Adv. Eng. Mat., Vol. 4 (2002), p. 735

[17] S.A. Koehler, S. Hilgenfeldt, E.R. Weeks and H.A. Stone, Physical Review E, 66 040601(R) (2002)